View metadata, citation and similar papers at core.ac.uk
brought to you by CORE
provided by Northumbria Research Link

Optimisation of oar blade design for improved performance in rowing

Nicholas Caplan[1] and Trevor N Gardner[2]

1. *School of Psychology and Sport Sciences, Northumbria University, Wynne Jones Centre, Ellison Place, Newcastle upon Tyne, NE1 8ST. UK*

2. *Biomechanics Research Group, School of Sport and Exercise Sciences, University of Birmingham, Edgbaston, Birmingham, B15 2TT. UK*

Correspondence to:

N Caplan
Division of Sport Sciences
Northumbria University
Wynne Jones Centre
Ellison Place
Newcastle upon Tyne
NE1 8ST
United Kingdom

Telephone +44 (0)191 243 7382
Fax +44 (0)191 227 4713
Email nick.caplan@northumbria.ac.uk

Abstract

The aim of the present study was to find a blade design more optimised for rowing performance than the Big Blade, which has been shown to not be fully optimised for propulsion. As well as the Big Blade, a flat Big Blade, a flat rectangular blade and a rectangular blade with the same curvature and projected area as the Big Blade were tested in a water flume to determine their fluid dynamic characteristics at the full range of angles at which the oar blade might present itself to the water. Similarities were observed between the flat Big Blade and rectangular blades. However, the curved rectangular blade generated significantly more lift in the angle range 0-90 ° than the curved Big Blade, although was similar between 90–180 °. This difference was attributed to the shape of the upper and lower edges of the blade and their influence on the fluid flow around the blade. Although the influence of oar blade design on actual boat speed was not investigated here, the significant increases in fluid force coefficients for the curved rectangular blade suggest that this new oar blade design could elicit a practically significant improvement in rowing performance.

Introduction

In rowing large forces are applied to the boat by the rowers in an attempt to propel the boat at a high velocity over a race distance typically of 2000 m. These forces originate at the foot stretcher through powerful extension of the rower's legs, and are transferred to the oar handle through the upper body from the pelvis to the hands remaining locked. The oar handle is then rotated about the oarlock, leading to some movement of the oar blade through the water. It is this relative movement between the oar blade and water that generates propulsive force.

In order for the forces applied by the rower to be optimised, the oar blade must be designed in such a way as to maximise its ability to generate both lift and drag forces throughout the rowing stroke (Affeld *et al*., 1993). Nolte (1984) first suggested that the oar blade movement through the water generates these forces in a similar way to an aerofoil, and by describing the movement of the oar blade in four phases, as previously presented by Dreissigacker and Dreissigacker (2000), the orientations of both lift and drag forces can be seen (Fig. 1). As illustrated in Fig. 1, lift forces dominate during the early phases of the stroke, causing the oar blade to move forwards in the water, with drag forces increasing as the oar shaft approaches a perpendicular position relative to the shell. Finally lift again dominates as the stroke nears the finish, or the end of the drive phase.

Until now, oar blade design has progressed mainly through trial and error (Pinkerton, 1992). In order to fully appreciate the ability of oar blades to generate both lift and drag forces in an attempt to optimise oar blade design, an understanding of the fluid

dynamic characteristics of oar blades must be gained. Lift force, F_L, and drag force, F_D, can be modelled as,

$$F_L = \frac{1}{2} C_L \rho A V^2 \quad (1)$$

and

$$F_D = \frac{1}{2} C_D \rho A V^2 \quad (2)$$

where ρ is the fluid density, A is the projected area of the oar blade measured perpendicularly to the face of the blade, and V is the relative velocity between the oar blade and water (Munson *et al.*, 2002). C_L and C_D are dimensionless force coefficients which are dependent upon the oar blade shape and the angle of attack between the oar blade chord line and the direction of fluid flow past the blade. In order to compare the fluid dynamic characteristics of different oar blade designs, it is therefore appropriate to calculate and compare the force coefficients in order to discount any influence of relative fluid velocity, fluid density, and blade size.

Caplan and Gardner (2005) presented a method for determining the force coefficients of model oar blades in a water flume using a quasi-static approach similar to that used in both swimming and kayaking research (Berger *et al*., 1995; Sumner *et al*., 2003). It was shown that the data was independent of Reynolds number above 9.44×10^4 (Caplan & Gardner, 2006) which agreed well with previously published data (Berger *et al*., 1995; Bixler & Riewald, 2002). It was also shown that the Big Blade oar blade design, although having similar lift and drag coefficients when the angle of attack between the oar blade and water was between 90–180 °, did not perform significantly better than a simple flat equivalent of the Big Blade at angles of attack below 90 °

(Caplan & Gardner, 2006). This led the authors to look more closely at aerofoil theory in an attempt to understand why this lack of difference in blade performance existed.

Caplan and Gardner (2006) suggested that the lack of difference in blade performance between the flat and curved Big Blades at low angle of attack was due to the shape of the upper and lower edges of the blade. During the second half of the stroke (Phase 4, Fig. 1), the shaft end of the blade will be the leading edge. As can be seen in Fig. 2, the vertical distance between the upper and lower edges increases as the water moves along the blade surface from shaft to tip (from right to left in Fig. 2). As such, it acts in a similar way to a delta wing as described by Hoerner and Borst (1985), and by generating strong lateral edge vortices (upper/lower edge for oar blade) which help to keep the water attached to the back surface of the blade, an increase in lift coefficient is generated with blade curvature, with blade curvature acting to increase boundary layer circulation which generates lift. However, during the first half of the stroke when the tip of the blade is the leading edge presented to the water, the distance between the upper and lower edges quickly drops away. Hoerner and Borst (1985) suggested that if this distance reduces moving from tip to trailing edge, the blade is unable to generate sufficient lateral edge vortices to maintain laminar flow across the back of the blade, so lift is not increased with blade curvature.

As the rowing stroke involves the oar blade being oriented over a large range of angles such that both the tip and shaft end of the blade are alternating as the leading edge presented to the water, a delta wing shaped blade cannot be an optimised design. Therefore, the aims of the present investigation were to determine the fluid dynamics

characteristics of a curved rectangular blade and compare them with those of a Big Blade. The curved rectangular blade has the upper and lower surfaces running parallel, thus removing the limitation of the current Big Blade discussed above. It was hypothesised that the rectangular blade would generate higher lift coefficients during the 0–90 ° range where it is suggested that the Big Blade is inefficient in generating lift.

Method

Oar blades

The fluid dynamic tests were performed in a water flume which had a free stream width and depth of 0.64 m and 0.15 m, respectively. Due to the inherent edge resistance effects on the on fluid flow, it was decided that quarter scale oar blade models should be used so that the length of the blades were less than a quarter of the flume width and remained in the part of the flume where velocity reductions arising from edge effects were minimal. The model blades were fabricated from 1.8mm thickness aluminium sheet, which was shown by dimensional analysis to provide sufficient stiffness to be able to discount any influence of oar blade bending. Although this model blade thickness is equivalent to an actual blade thickness of 7.2 mm, rather than 5 mm for an actual Big Blade, blade thickness is considered not to have a significant influence on blade performance compared to shape and surface area of the blade. A number of oar blade designs were tested including a flat rectangular blade and a curved rectangular blade with curvature matching that of the previously

presented Big Blade (Caplan & Gardner, 2006). A second curved rectangular blade was also tested with the maximum depth of curvature increased from 10 mm to 15 mm. The fluid dynamic characteristics of these blade designs were then compared to those of the Big Blade.

Experimental setup

In order to measure the forces being applied to the oar blade models, a measurement system was designed such that the model blades could be held static in the flume at a range of angles relative to the direction of free stream. The blades were attached to a model oar shaft, such that their orientations matched that of the Big Blade, and the model shaft made an angle of 10 ° with the water surface. This model oar shaft was attached to a vertical bar, and strain gauges were located on both the oar shaft and vertical bar in order to record the normal and tangential fluid forces generated by the model oar blades (Fig. 3).

This allowed for the determination of lift and drag forces using the equations,

$$F_{Lift} = F_T \sin\alpha + F_N \cos\alpha \quad (3)$$

and

$$F_{Drag} = F_N \sin\alpha - F_T \cos\alpha \quad (4)$$

where F_T is the blade force acting tangentially to the blade chord line, F_N is the blade force acting normally to the blade chord line and α is the angle of attack between the

blade chord line and the free stream direction of fluid flow (Fig. 4). The angular position of the vertical bar in the horizontal plane, and hence the angle α of the oar shaft, was measured using a 360 ° smart position sensor (601-1045, Vishay Spectrol, UK), which had a stated linearity of ±1 % and a resolution of 0.5 °. This position sensor was powered by a fixed voltage power supply (5 V), and the output of the position sensor was displayed on a digital volt meter. For a detailed description of the design and calibration of the measurement system, and the reduction of lift and drag forces from the strain gauge recordings, see Caplan and Gardner (2005).

Influence of Reynolds number

As with any fluid dynamic test involving the use of scaled models, both geometric (aspect ratio) and dynamic (Reynolds number) similarity must be achieved in order for the model data to be directly applied to the real life situation. As the models were scaled exactly from the full size oar blades, geometric similarity was met. However, due to the scale of the models and the maximum velocity that could be achieved by the water flume, it was not possible to gain Reynolds number similarity. It was therefore necessary to determine the Reynolds number dependence of the lift and drag coefficients. Reynolds number is given by

$$\mathrm{Re} = \frac{\rho V l}{\mu} \qquad (5)$$

where ρ is the fluid density, V is the fluid velocity, l is a characteristic length of the object, and μ is the kinematic viscosity of the fluid (Munson *et al.*, 2002). The

dependence of the model data on Reynolds number can therefore be determined by varying either the model size or relative free stream velocity. Due to the edge effects of the water flume, with the fluid velocity reducing as the edges are approached, the measured force coefficients would be influenced by a reduced average free stream velocity across the frontal area of the blade if the blade size was increased. Therefore, the flat plate, the simplest of blade designs, was tested at a range of fluid velocities, between 0.4 - 0.85 $m.s^{-1}$ using the protocol described above. It was found that lift and drag coefficients were independent of Reynolds number with a free stream velocity above 0.7 $m.s^{-1}$ (see Caplan & Gardner, 2006a). A fluid velocity of 0.75 $m.s^{-1}$ was therefore used for the remainder of the tests, which was high enough to overcome any influence of Reynolds number, but not so high that the increasing turbulence of the water interfered with the measurement system.

Experimental protocol

Before each blade was tested, reference flow conditions were established by making a point velocity measurement at a depth of 25 mm from the water surface in the centre of the flume using a miniature current flowmeter probe (403, Nixon, UK), and the rotational frequency of the probe was displayed on a flow meter (Streamflo 400, Nixon, UK).

A ten second base line force measurement was taken and the data averaged over the duration of this period. The oar blade was then placed in the flume so that the blade chord line was in line with the direction of free stream ($\alpha = 0$ °), and with the top edge

of the blade flush with the water surface. Signals from the strain gauges passed through a custom made strain gauge amplifier before passing to an analogue-digital card (PC-DAS 16/12, Measurement Computing, USA), which sampled the data at a frequency of 2.5 kHz for a period of 15 seconds for each trial. The angle of attack was increased in 5 ° intervals between 0 – 180 °. Four 15 second trials were collected at each angle of attack.

The data collected during each 15 second collection period was averaged to provide four mean voltages for each strain gauge bridge at each angle. These voltages allowed for the calculation of lift and drag forces as described earlier. The water temperature was measured at 16 °, which equated to a fluid density of 999 kg.m^3.

A macro image analyser (Carl Zeiss, Germany), was used to photograph the blades from directly above and the software Axio Vision (Carl Zeiss, Germany), was subsequently used to determine the projected area of each blade image shown in Table 1. These values, along with the fluid density, the measured fluid velocity and lift and drag forces were substituted into equations (1) and (2) to provide lift and drag coefficients for each angle of attack.

Table 1. Projected areas for the model oar blades tested.

Blade Description	**Projected Area (cm^2)**
Flat Big Blade	77.42
Curved Big Blade	77.41
Flat Rectangular Blade	77.37
Curved Rectangular Blade	77.52
Curved Rectangle (↑curvature)	77.82

Data analysis

The calculated lift and drag coefficients were compared between oar blade designs. Independent samples t-tests were used at each angle, α, to determine if the difference between oar blade designs was significant, with a 99 % confidence level ($P<0.01$) being used throughout.

Results and Discussion

Figure 5 compares the shaped (Big Blade) and rectangular flat blades. Both C_D and C_L were similar for both blades. C_L appeared to be slightly, but not significantly, increased for the rectangular blade between 20-45 ° and was significantly increased between 135-145 °. This can be explained by low aspect ratio wing theory presented by Hoerner and Borst (1985). The authors stated that with wings, or oar blades, of aspect ratio (width/height) less than 3 the lateral edges, and in the case of oar blades the top and bottom edges, play a significant role in the generation of lift. In a normal wing, the fluid flows over the upper and lower surfaces and the orientation of the wing to the fluid flow results in circulation of the boundary layer, or the fluid particles attached to the surface of the wing, and this circulation causes a change in momentum of the boundary layer which in turn generates a lifting force. As the angle of attack is increased, the boundary layer will start to separate away from the back surface of the

wing causing turbulent flow and at an angle of attack around 15 °, the turbulent flow will dominate and lift force will decrease or stall.

For low aspect ratio wings, however, the lateral edges of the wing play an important role. Due to their proximity to the centre line of the wing, there will be a large amount of flow that moves laterally away from this centre line and will "spill" over the lateral edges. Vortices are then generated along these edges which help the fluid remain attached to the back of the wing, thus delaying the onset of stall and loss of lift. With a rectangular blade, the straight edges help to increase the magnitude of these lateral edge vortices, delaying the onset of separation, thereby increasing lift. With the Big Blade, the design is such that the width of the blade (or the vertical dimension of the blade) reduces as the fluid flows from the tip to shaft, thus reducing the aspect ratio and losing the blade's effectiveness at generating lateral edge vortices.

It has been shown previously that the potential increase in lift due to blade curvature for the Big Blade design was not observed at angles of attack less than 90 °, and this was attributed to the shape of the upper and lower edges of the blade (Caplan & Gardner, 2006). To test this hypothesis further, flat and curved rectangular blades were compared. Since the two blades have the same aspect ratio and both have parallel edges, any differences in performance will be due to the curvature only. Figure 6 shows this to be the case, with significant increases in lift being seen with curvature between 0-15 °, 40-70 ° and at most angles between 90-180 °. It was expected that C_D would be increased with the curved blade at angles around 90 ° due to the water becoming trapped on the face of the blade as it behaves like a spoon (Bird, 1975); in fact significant increases were seen at most angles of attack.

If lift can be increased significantly between flat and curved rectangular blades, while the increase between flat and curved Big Blades was shown to be similar at angle of attack below 90 °, then would a curved rectangular blade be a more efficient blade design for the generation of lift during the rowing stroke compared to the curved Big Blade? Figure 7 compares the curved Big Blade to the curved rectangular blade. C_L was observed to be significantly increased at nearly all angles up to 140 °. However, C_L was similar for the two blades above 140 ° and significantly greater for the Big Blade at 175 °. It is suggested that the increased lift seen at these angles is due to the curved Big Blade acting like a delta wing as described earlier.

C_D was significantly increased for the curved rectangular blade at most angles of attack between 0-70 °. This is most likely due to the shape of the top edge of the blade. In the rectangular blade, this edge runs parallel to the surface of the water and the water must be lifted over the entire length of this edge. With the shaped blade, the top edge is curved in the vertical plane, dropping away as you move away from the vertical blade centre line. Therefore, the water will only have to be lifted to the same extent as the rectangular blade at the blade centre, and less energy for lifting water will be required as it approaches the sides. Both blades produced similar C_D between 75-150 °, with C_D being significantly increased for the Big Blade above 155 °.

Caplan and Gardner (2006) previously compared the fluid dynamics of the Big Blade to the Macon oar blade design, which was the most commonly used blade design until 1991. The Big Blade has been suggested to increase performance by approximately two percent compared to the Macon (Affeld *et al.*, 1993; Dreissigacker &

Dreissigacker, 2000), despite the lack of fluid dynamic differences reported by Caplan and Gardner (2006). Therefore, the significant increases in lift coefficient seen here between the Big Blade and the curved rectangular blades during the first half of the stroke have the potential to make a practically significant difference to rowing performance.

As discussed above, blade curvature significantly increases the magnitude of lift force generated by the blade through increasing circulation of the fluid boundary layer around the oar blade, and it increases drag force through increased pooling of the fluid on the face of the blade. This, therefore, raises the question as to whether the increases in lift and drag observed can be increased further by increasing the amount of blade curvature. Figure 8 shows lift and drag coefficients for the curved rectangular blade presented above compared to a rectangular blade when depth of curvature was increased from 10 mm to 15 mm.

Visual inspection of the C_L curves suggests that at angles of attack up to 50 ° C_L is increased. However, this increase was not significant except at 20 °, and at most angles above 90 ° C_L was greater for the blade with less curvature. As was shown previously (Caplan & Gardner, 2006) for the flat and curved shaped blades at angles of attack below 90°, the curved blade produced no more lift than the flat blade. It was suggested that this was due to the lateral edge vortices being unable to keep the fluid flow bound to the back of the blade to compensate for the increased fluid separation that occurs with curved blades compared with straight ones. It is believed that the same effect occurred here. As the depth of curvature is increased, more fluid separation will occur away from the back of the blade, and the magnitude of the

lateral edge vortices must be increased in order for the flow to remain attached. The lack of differences in C_L suggested that the magnitude of the lateral edge vortices was not sufficient to prevent fluid separation. It is likely, therefore, that blade curvature can be increased to some optimum curvature, above which fluid separation will cause C_L to plateau or decrease. C_D was observed to be similar between the two blades at most angles of attack, being significantly increased for the more curved blade above 160 °. If the blade is observed from an upstream position when the blade is at an angle of attack of 180 °, as the depth of curvature increases the visible area of the blade as seen by the oncoming water will increase, which will result in an increase in form drag at similar angles of attack, thus producing a higher C_D.

Conclusion

A number of different oar blade designs were compared, showing that blade curvature is important for maximising both lift and drag forces. The design of the Big Blade was shown to be close to optimal during the second half of the stroke, when the shaft end of the blade is the leading edge. However, a simple curved rectangular blade was shown to generate significantly higher lift coefficients at angles of attack less than 90 °, suggesting that rowing performance could be improved. However, although an improvement in performance was postulated for the curved rectangular blades, with the increases in fluid force coefficients being much greater than those seen previously between the Big Blade and Macon blade designs (Caplan & Gardner, 2006), an optimal depth of curvature was not determined. In order to fully optimise both the shape and depth of blade curvature, a complex computational fluid dynamic (CFD)

investigation would be required. The present tests ignored the blade entry and exit phases at the catch and finish of the stroke, respectively, and this could have a limiting effect on blade design. However, the potentially large improvements in blade performance suggested here would likely outweigh any negative influences of blade design on blade entry at the catch or finish of the stroke. In order to examine the influence of oar blade design on rowing performance, the fluid force coefficients from either the experimental trials, or any future CFD models, would need to be used as inputs to a mathematical model of rowing to predict the practical significance of changing blade shape on rowing performance.

Reference List

Affeld, K., Schichl, K., & Ziemann, A. (1993). Assessment of rowing efficiency. *International Journal of Sports Medicine, 14 Suppl 1*, S39-S41.

Berger, M. A., de Groot, G., & Hollander, A. P. (1995). Hydrodynamic drag and lift forces on human hand/arm models. *Journal of Biomechanics, 28,* 125-133.

Bird, W. J. (1975). The mechanics of sculling. *Chartered Mechanical Engineer, 22,* 91-94.

Bixler, B. & Riewald, S. (2002). Analysis of a swimmer's hand and arm in steady flow conditions using computational fluid dynamics. *Journal of Biomechanics, 35,* 713-717.

Caplan, N. & Gardner, T. N. (2005). A new measurement system for the determination of oar blade forces in rowing. In *Proceedings of the XXth IASTED International Symposium on Biomechanics* (edited by Hamza, M.H.). Calgary: ACTA Press.

Caplan, N. & Gardner, T. N. (2006). A fluid dynamic investigation into the Big Blade and Macon oar blade designs in rowing propulsion. *Journal of Sports Sciences,* (In press).

Dreissigacker, D. & Dreissigacker, P. (2000). Oars - Theory and Testing, XXIX FISA Coaches Conference Sevilla, Spain.
http://www.oarsport.co.uk/oars/c2_vortex_development.php. [Accessed: 26/09/06]

Hoerner, S. F. & Borst, H. V. (1985). *Fluid-dynamic lift*. (2 ed.) Albuquerque, New Mexico: Hoerner Fluid Dynamics.

Kleshnev, V. (1999). Propulsive efficiency of rowing. In *XVII International Symposium on Biomechanics in Sports* (edited by R.H.Sanders & N. R. Gibson), pp. 224-228, Perth: ECU

Munson, B. R., Young, D. F., & Okiishi, T. H. (2002). *Fundamentals of fluid mechanics*. (4th ed.) New York: John Wiley & Sons, Inc.

Nolte, V. (1984). *Die effektivitat des ruderschlages*. Berlin: Bartels & Wernitz.

Pinkerton, P. (1992). The Big Blade goes big time. *Australian Rowing, September*, 10-11.

Sumner, D., Sprigings, E. J., Bugg, J. D., & Heseltine, J. L. (2003). Fluid forces on kayak paddle blades of different design. *Sports Engineering, 6,* 11-20.

Figure 1

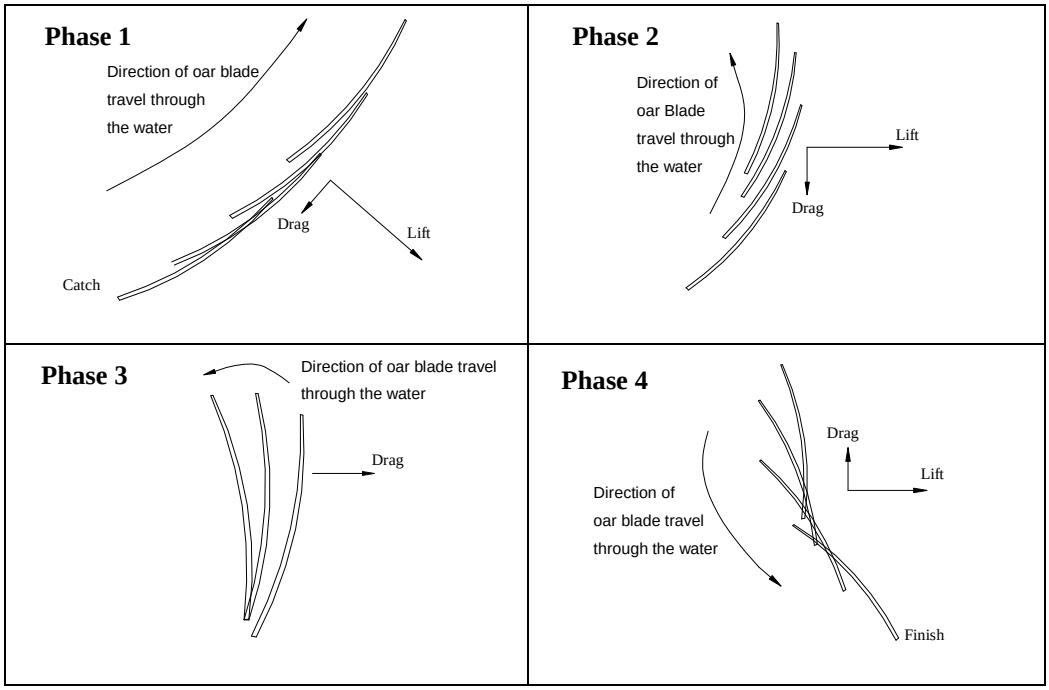

Figure 1. The movement of a right handed oar blade during the drive phase of the rowing stroke with the boat moving from left to right. The approximate directions of the lift and drag forces generated are indicated (adapted from Dreissigacker & Dreissigacker (2000)).

Figure 2

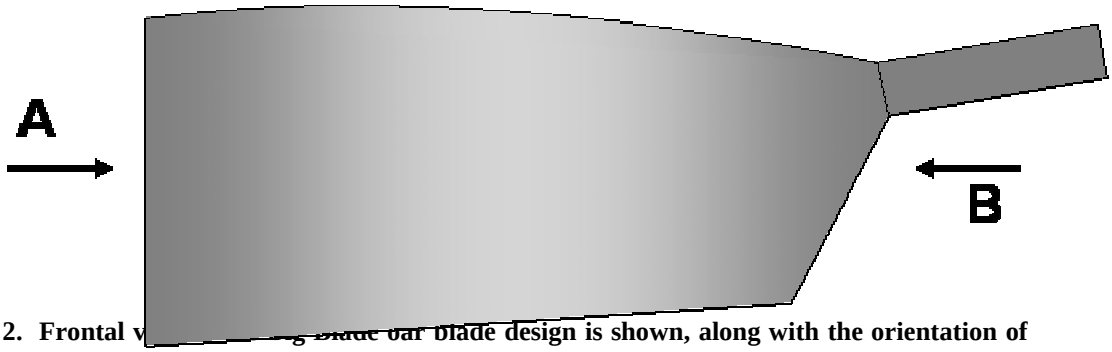

Figure 2. Frontal v[illegible] blade oar blade design is shown, along with the orientation of oar shaft attachment. 'A' shows the leading edge during the first half of the drive phase of the stroke, and 'B' shows the leading edge during the second half.

Figure 3

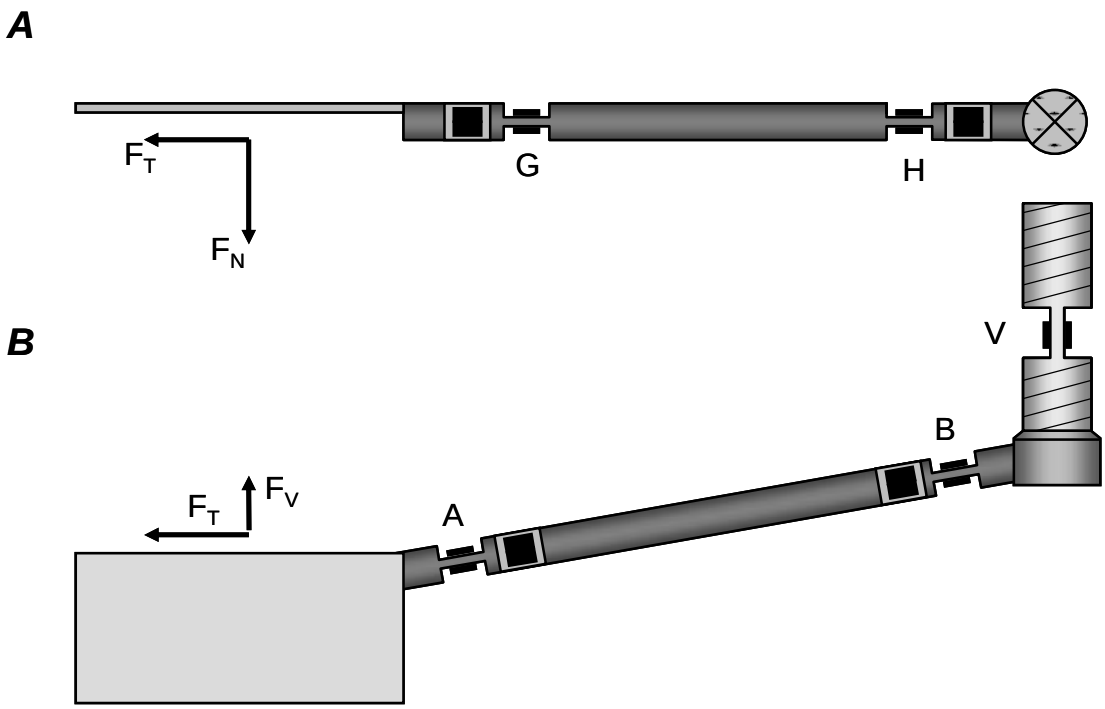

Figure 3. Plan (A) and side (B) views of the measurement system used to measure the normal and tangential oar blade forces, through the use of strain gauges A, B, G, H and V (Caplan & Gardner, 2005).

Figure 4

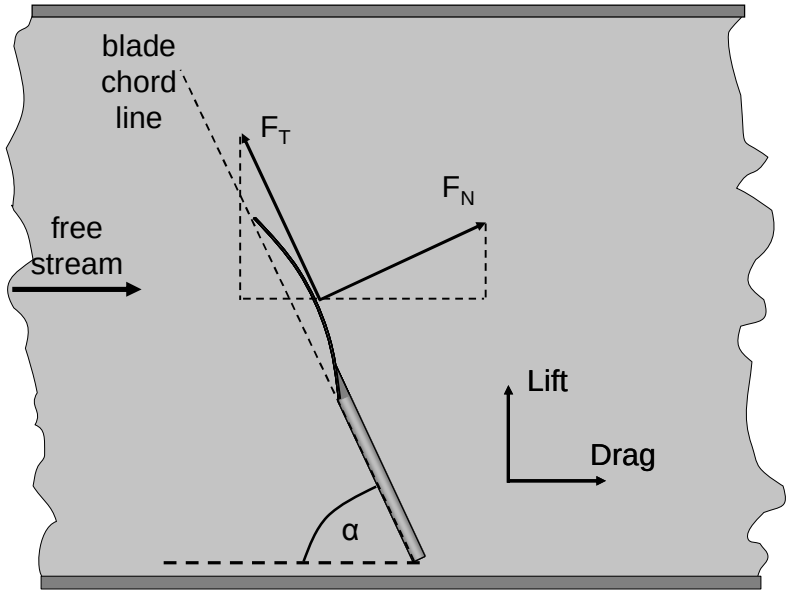

Figure 4. Plan view of the water flume showing the orientation of the oar blade. The direction of lift and drag forces are illustrated, along with the measured normal and tangential oar blade forces and the chord line of the blade.

Figure 5

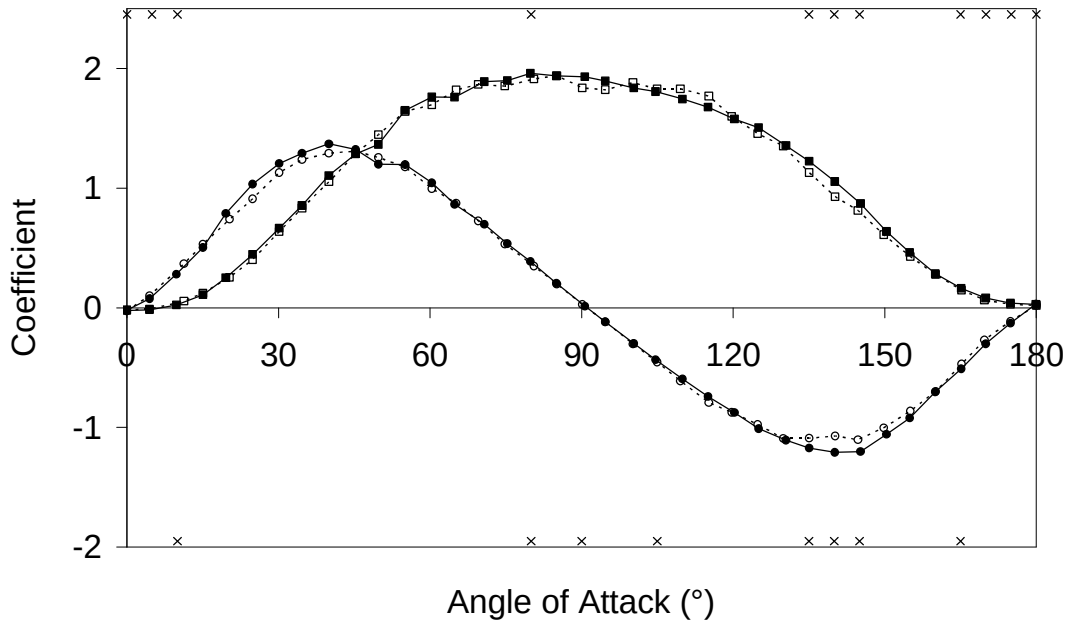

Figure 5. Lift (●/○) and drag (■/□) coefficients are compared for the flat rectangular (─) and flat Big Blade (---). x at the top of the figure signifies significant differences between blade designs for drag coefficient and along the bottom of the figure for lift coefficient ($P < 0.01$).

Figure 6

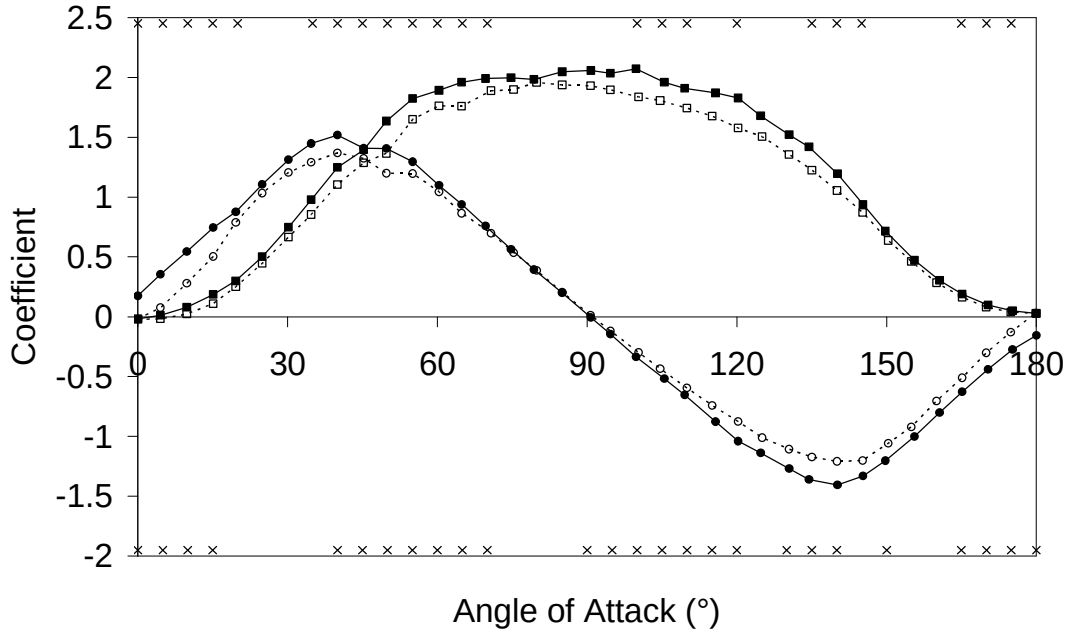

Figure 6. Lift (●/○) and drag (■/□) coefficients are compared for the flat (---) and curved (─) rectangular blade. x at the top of the figure signifies significant differences between blade designs for drag coefficient and along the bottom of the figure for lift coefficient ($P < 0.01$).

Figure 7

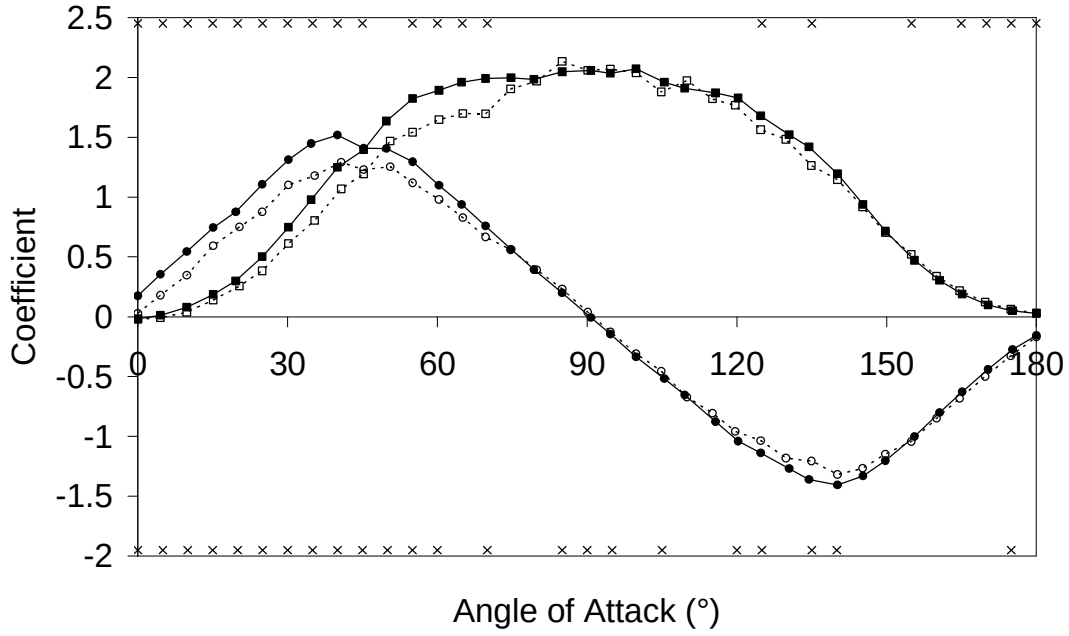

Figure 7. Lift (●/○) and drag (■/□) coefficients are compared for the curved Big Blade (---) and curved rectangular blade (—). x at the top of the figure signifies significant differences between blade designs for drag coefficient and along the bottom of the figure for lift coefficient ($P < 0.01$).

Figure 8

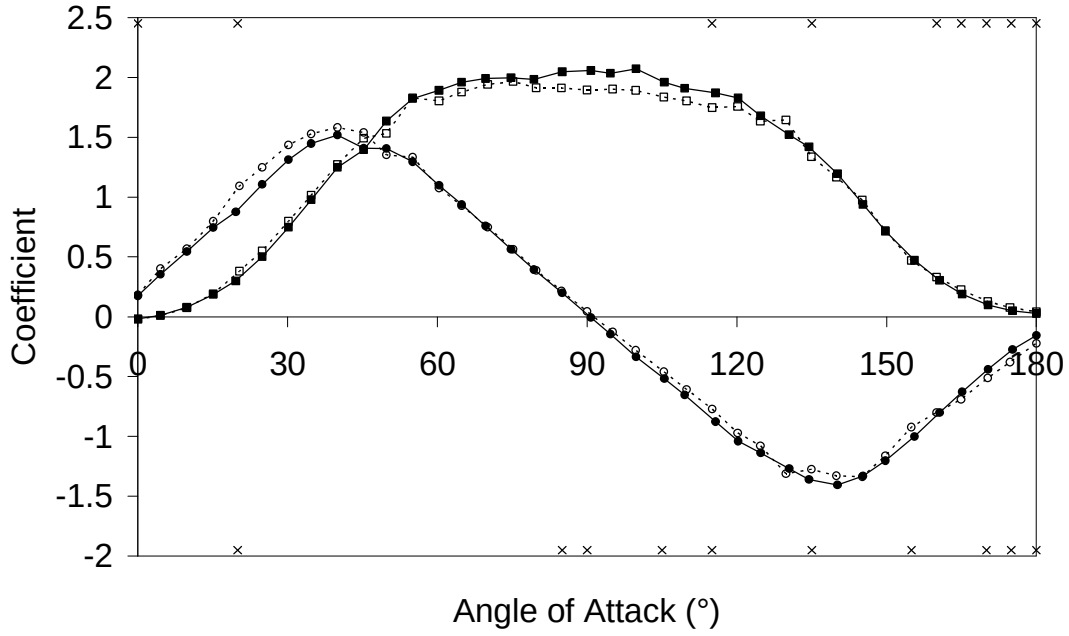

Figure 8. Lift (●/○) and drag (■/□) coefficients are compared for the curved rectangular blade (—) and the same blade with increased depth of curvature (---). x at the top of the figure signifies significant differences between blade designs for drag coefficient and along the bottom of the figure for lift coefficient ($P < 0.01$).